Stand-off molecular composition analysis

Gary B. Hughes[a], Philip Lubin[b], Peter Meinhold[b], Hugh O'Neill[c], Travis Brashears[b], Qicheng Zhang[b], Janelle Griswold[b], Jordan Riley[b] and Caio Motta[b]
gbhughes@calpoly.edu
[a]Statistics Department, California Polytechnic State University, San Luis Obispo, CA 93407
[b]Physics Department, University of California, Santa Barbara, CA 93106
[c]Physics Department, Ventura College, Ventura, CA 93003

ABSTRACT

Composition of distant stars can be explored by observing absorption spectra. Stars produce nearly blackbody radiation that passes through the cloud of vaporized material surrounding the star. Characteristic absorption lines are discernible with a spectrometer, and atomic composition is investigated by comparing spectral observations with known material profiles. Most objects in the solar system—asteroids, comets, planets, moons—are too cold to be interrogated in this manner. Material clouds around cold objects consist primarily of volatiles, so bulk composition cannot be probed. Additionally, low volatile density does not produce discernible absorption lines in the faint signal generated by cold objects. We propose a system for probing the molecular composition of cold solar system targets from a distant vantage. The concept utilizes a directed energy beam to melt and vaporize a spot on a distant target, such as from a spacecraft orbiting the object. With sufficient flux (~10 MW/m^2) on a rocky asteroid, the spot temperature rises rapidly to ~2500 K, and evaporation of all materials on the surface occurs. The melted spot creates a high-temperature blackbody source, and ejected material creates a molecular plume in front of the spot. Bulk composition is investigated by using a spectrometer to view the heated spot through the ejected material. Spatial composition maps could be created by scanning the surface. Applying the beam to a single spot continuously produces a borehole, and shallow sub-surface composition profiling is possible. Initial simulations of absorption profiles with laser heating show great promise for molecular composition analysis.

Keywords: DE-STAR, Directed Energy, Laser Phased Array, Planetary Defense

1. INTRODUCTION

1.1. Composition of Solar System Objects

Composition of distant stellar and sub-stellar objects is explored by observing absorption spectra.[1] The (hot) object being studied produces blackbody radiation that passes through the cloud of vaporized material surrounding the object. Characteristic absorption lines are discernible with a spectrometer, and atomic composition of the cloud is investigated by comparing spectral observations with known material profiles.[2] Most objects in the solar system—asteroids, comets, planets and moons—are too cold to be interrogated in this manner. Material clouds around cold objects consist primarily of volatiles, so bulk composition cannot be probed. Additionally, low volatile density does not produce discernible absorption lines in the faint signal generated by the low blackbody temperatures of cold objects (composition of volatiles can sometimes be surveyed as the object transits a star). Bulk composition of cold objects is currently investigated using indirect methods, such as by inference from thermal properties, or through direct measurement by a suitably-equipped lander. This paper describes a conceptual system that is capable of probing the molecular composition of cold solar system targets such as asteroids, comets, planets and moons from a distant vantage. The proposed concept utilizes a directed energy beam to melt and vaporize a spot on a distant target, such as from a spacecraft orbiting the object. With sufficient flux (~10 MW/m^2), the spot temperature rises rapidly (to ~2 500 K), and evaporation of all materials on the target surface occurs.[3] The melted spot serves as a high-temperature blackbody source, and ejected material creates a molecular plume in front of the spot. Bulk composition is investigated by using a spectrometer to view the heated spot through the ejected material. A

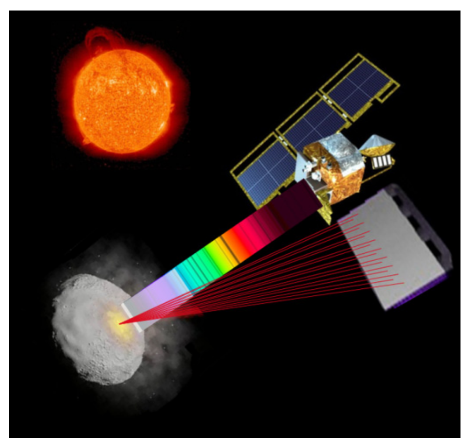

Figure 1. Conceptual drawing of a proposed laser ablation system for remote composition analysis.

spacecraft could be sent to probe the composition of a target asteroid, comet or other planetary body while orbiting the targeted object, as depicted in Fig. 1. Spatial composition maps could be created by scanning the directed energy beam across the surface. Applying the laser beam to a single spot continuously produces a borehole, and shallow sub-surface composition profiling is also possible. Initial simulations of absorption profiles with laser heating show promise for molecular composition analysis. Such a system has compelling potential benefit for solar system exploration by establishing the capability to directly interrogate the bulk composition of objects from a distant vantage. This paper describes theoretical models of plume density created by laser ablation, and estimates of optical thickness and molecular absorption are used to assess the viability of remote molecular composition analysis.

1.2. Comparison to Existing Methods

As described above, the current approach for querying the composition of distant targets requires the target itself to provide a strong blackbody source, so cold targets are not accessible. Other technologies are available for measuring the atomic composition of materials over very modest distances in the field, such as by Laser-Induced Breakdown Spectroscopy (LIBS) or Laser-Induced Thermal Emission (LITE).[4,5] With these methods, a laser pulse is focused on the sample, with sufficient energy flux to form a plasma, which atomizes and ionizes materials in the target. The scattered ions then emit characteristic radiation, allowing atomic composition analysis (but not the parent molecular composition) by observing emission spectra. Characteristic emission is faint, requiring the sensor to be in close proximity to the target, so LIBS and LITE methods are not scalable to large distances. For example, in order to interrogate the composition of a planetary body, a landing mission would be required. Furthermore, atomic composition determined from ionized materials does not always yield information about chemical formula units. With the proposed system described in this paper, stand-off distance is only limited by the ability to point and focus a directed energy beam on the target, and by the opacity of the ejected material plume. Results presented in this paper indicate that, with currently available technology, stand-off molecular composition analysis is feasible over distances greater than 100 km and over much greater distances with modest advances in optical systems.[3]

1.3. Additional System Capabilities

The ability to probe molecular composition of cold objects from a distant vantage would represent a great leap in capabilities over existing technologies. The primary objective of the proposed system would be stand-off molecular composition analysis of solar system bodies, *e.g.*, in a scenario such as NASA's proposed Asteroid Retrieval Mission (ARM).[6] A hypothetical mission for such a system might be to perform high spatial resolution surface bulk molecular composition analysis and mapping of a near-Earth asteroid (NEA). Proposed system architecture includes using a directed-energy beam to heat a spot on the asteroid to the vaporization point of crustal rocks, and to capture high-fidelity spectral measurements for molecular compositional analysis. With such a system, additional science objectives could also be pursued. The ejected plume creates a reactionary thrust that could be exploited for orbit alteration in impact avoidance scenarios or asteroid capture missions. Numerous studies have confirmed the efficacy of low-thrust approaches using laser ablation for orbit alteration.[3,7,8,9,10] An Earth-orbiting directed energy system could be used for debris mitigation, for example by mounting a directed energy system on the International Space Station. Directed energy beams could also be used for beamed power delivery, including beamed propulsion for solar system missions.[11] The proposed system could be used in a 'search-LIDAR' scanning mode to illuminate dark targets, and could aid discovery of smaller near-Earth asteroids that are increasingly difficult to detect with passive sensors.[12,13]

2. THERMAL ANALYSIS

2.1. Laser Heating

The core idea of remote composition analysis relies on the ability to heat a distant target to the point of vaporization. Advances in laser technology now allow contemplation of systems that are capable of delivering sufficient flux to vaporize very distant targets. The performance of Ytterbium-doped fiber laser amplifiers has improved markedly in recent years. Continuous-wave, multi-kW-class devices are now routine and affordable, germinating many novel applications.[14] Phased array configurations of laser fiber amplifiers have been demonstrated in the laboratory.[15,16,17,18,19] Modular designs that could be constructed and extended in orbit have also been proposed.[20] Alternatively, multiple lasers could be arranged without phase alignment, and individual beams could be focused on adjacent spots on the target. Multi-beam configurations are effective, but would be limited to closer targets than phased-array emitters with equivalent base power.

A multi-physics model of the thermal progression of a bolide being bombarded with laser energy has been developed, including a detailed derivation of the model.[3,10] The thermal model was derived from energy conservation, and includes thermal characteristics of the bolide being bombarded with laser energy. Numerical implementations of the model are used to run simulations, both with phase-locked laser arrays as the illuminating source, and with phase-independent multi-beam configurations. Model results indicate a solid theoretical foundation supporting the proposed method.[3,10,21,22,23] The model suggests that vaporization commences within 1 second; the thermal profile stabilizes at a level consistent with the vaporization temperature of Silica in vacuum. Temperatures within the illuminated spot rise to the point of being mass ejection limited, which is ~2 250 K in the center of the spot. Results of a simulated run are shown in Fig. 2.[21,23]

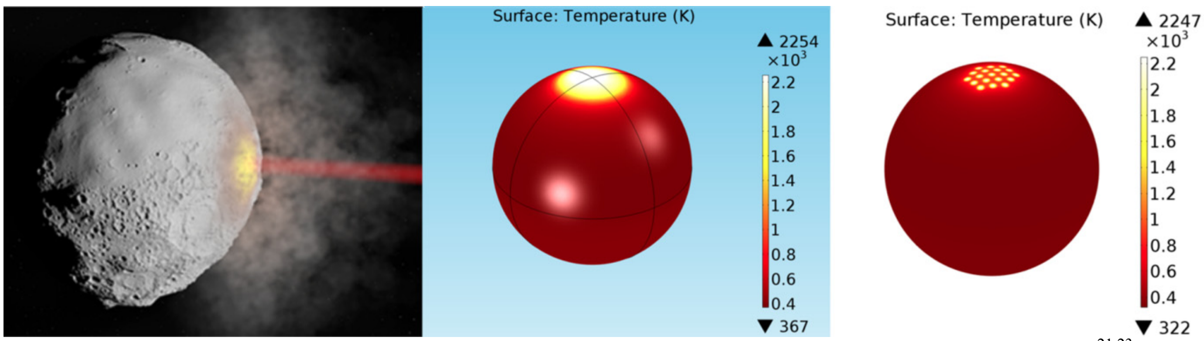

Figure 2. Results from a multi-physics model of a spherical bolide of micro-crystalline Silica (SiO_2).[21,23] Model features include radiation, conduction and mass ejection. **Left:** Conceptual illustration of a directed energy beam impinging on an asteroid; surface material is ejected from the heated spot, creating a plume. **Center:** Simulation results showing steady-state condition, under illumination with a single beam produced by an array of phase-locked lasers. **Right:** The same bolide, under illumination with multi-beam emitter.

2.2. Surface Material Ejection

The energy required to vaporize materials on the surface of an asteroid is determined by the heat of fusion and required increase in temperature to bring the surface material to the melting point from (assumed) initial low temperature starting point. Fig. 3 shows the relationship between vapor pressure in Pascals (N/m^2) versus Temperature, and versus target flux, for several compounds that are thought to be common in asteroids.[3,10] The typical energy per m^3 is on the order of 10^{10} J to vaporize most materials. At temperatures exceeding ~2 250 K, which occurs at fluxes greater than ~10 MW/m^2, the vapor pressures of all compounds are very high. That is, none of these materials remain solid, and mass ejection rates will be high. Even vapor pressures in the range of 10^3 Pa (0.01 atmospheres) correspond to large mass ejection rates. The curves in Fig. 3 are applicable to the worst case of complete chemical binding (*i.e.*, solid). In contrast to the small iron-rich meteorites that are sometimes found on the ground, a more typical asteroid likely has much lower thermal conductivity, for example in cases where the asteroid is an agglomeration of smaller fragments (a "rubble pile" asteroid). In many cases asteroids, will have significant amounts of low temperature volatile materials that lower the power requirements for evaporation of surface material. Asteroids are also molecular rather than atomic in species in general, but the conclusion are the same, namely at temperatures in the range of 2 000 to 3 000 K or target fluxes in the range 106 to 108 W/m^2, all known materials will undergo vigorous evaporation. What is critical is to increase the spot flux to the point where evaporation becomes large. It is not sufficient to simply apply a large amount of total power, there has to be a large flux to initiate evaporation.

3. PHYSICS OF MASS EJECTION

3.1. Material Properties

Mass ejection from a solid that is heated is analogous to evaporation of a liquid, except in many circumstances the solid material is effectively sublimating. The effective vapor pressure of the material being ejected is essentially in equilibrium though in the case of an asteroid, surface evaporation or sublimation is a pure equilibrium process as the material streams into the hard vacuum of space. This process is similar but critically different than a constant temperature case where the mass ejection rate is temperature limited by the constant bath temperature. In the case of a laser beam striking the surface of an asteroid in space, the laser adds energy to the material and this is counteracted by the outgoing energy channels of surface reflection, scattering and absorption in the ejecta, mass ejection, radiation and thermal conductivity. This is somewhat different than the constant temperature case where the mass ejection stops increasing when the vapor pressure is limited by the temperature. The laser heats the material to the point where the increase in temperature is balanced by the energy loss due to all other processes. In particular the surface effects (Knudsen layer) are different as the temperature will increase to the point where energy equilibrium is achieved. This is different than the constant temperature case where thermal equilibrium at the constant temperature is achieved. Fig. 3 illustrates several cases for typical compounds present in asteroids both vs. temperature and flux. The analysis for each compound is calculated as below.

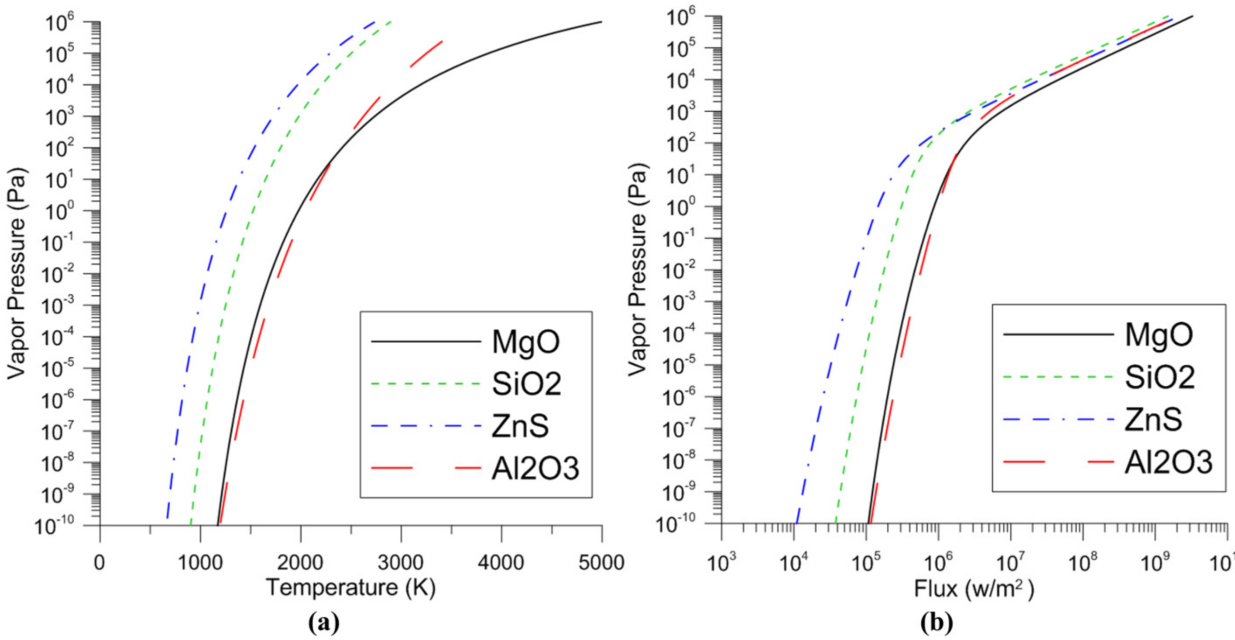

Figure 3. Vapor pressure relationship with temperature flux for several compounds that are thought to be common in asteroids.[3,10] **Left**: Vapor pressure vs. Temperature for selected compounds. **Right**: Vapor pressure vs. target flux for the same compounds.

3.2. Mass Ejection

To calculate the mass ejection, use Langmuir's equation for evaporation. The particle ejection rate, or evaporative flux, I_e (molecules m^{-2} s^{-1}) is given by:

$$I_e = \frac{\alpha_e (P_v - P_h)}{\sqrt{2\pi mkT}} = \frac{\alpha_e N_A (P_v - P_h)}{\sqrt{2\pi MRT}} \tag{1}$$

Symbols used in equations and text in this section are defined in Table 1. The mass flux Γ_ε (kg m^{-2} s^{-1}) is found from the Langmuir equation Eq. (1):

$$\Gamma_e = \mathrm{I}_e m = \frac{m\alpha_e (P_v - P_h)}{\sqrt{2\pi mkT}} = \frac{M\alpha_e (P_v - P_h)}{\sqrt{2\pi MRT}} = \alpha_e P_v \sqrt{\frac{M}{2\pi RT}} = \frac{\alpha_e P_v}{\upsilon_{AV}\pi / 2} = \frac{\alpha_e P_v}{\upsilon_e} \tag{2}$$

Alternatively,

$$\Gamma_e = \frac{M\alpha_e (P_v - \mathrm{P}_h)}{\sqrt{2\pi MRT}} = M^{1/2} (2\pi RT)^{-1/2} \alpha_e (P_v - \mathrm{P}_h) \tag{3}$$

Assuming the ambient pressure (P_h) is zero in vacuum, the average molecular speed is:

$$\upsilon_{AV} = \frac{8RT}{\sqrt{\pi M}} \tag{4}$$

Here, the effective speed (υ_ε) is defined to be:

$$\upsilon_e = \frac{\pi \upsilon_{AV}}{2} = \sqrt{\frac{2\pi RT}{M}} \tag{5}$$

Substituting the expression Eq. (5) into Eq. (2) gives

$$\Gamma_e \upsilon_e = \alpha_e P_v \tag{6}$$

This is effectively like rocket thrust $(dm/dt)\cdot\upsilon_\varepsilon$ except per unit area, so pressure:

$$P_v = \frac{\Gamma_e \upsilon_e}{\alpha_e} \tag{7}$$

where the expression $\Gamma_\varepsilon \cdot \upsilon_\varepsilon$ is the plume pressure. Rearranging terms gives:

$$\frac{\Gamma_e \upsilon_e}{P_v} = \alpha_e \tag{8}$$

The mass flux (in kg m^{-2} s^{-1}) is

$$\Gamma_e = 0.138\alpha_e \sqrt{\frac{M}{T}}(P_v - P_h) \tag{9}$$

Table 1. Terms used in equations and text in Section 3.

Symbol	Interpretation	Units
I_ε	Evaporative flux	Molecules m^{-2} s^{-1}
P_v	Vapor pressure	Pa
P_h	Ambient pressure (= 0 in vacuum)	Pa
α_ε	Coefficient of evaporation, $0 \le \alpha_\varepsilon \le 1$	unitless
m	Mass of molecule	kg
k	Boltzmann constant	m^2 kg s^{-2} K^{-1}
$M = mN_A$	Molar mass	kg mol^{-1}
$R = NA_k$	Constant, ≈ 8.31	unitless
Γ_ε	Mass flux	kg m^{-2} s^{-1}
T	Absolute temperature	K
$(T)_C$	Celsius temperature	°C
υ_ε	Effective molecular speed	m s^{-1}
υ_{AV}	Average molecular speed	m s^{-1}
$(P)_T$	Pressure	Torr
$(P)_{Hg}$	Pressure	mm Hg
H_v	Heat of vaporization (or sublimation)	J kg^{-1}
H_F	Heat of fusion	J kg^{-1}
F_L	Laser flux	W m^{-2}
L_P	Laser Power	W
F_{rad}	Outgoing radiation flux	W m^{-2}
F_{ejecta}	Outgoing mass ejecta flux	W m^{-2}
F_{cond}	Ingoing conduction flux	W m^{-2}
A, B and C	Antoine Coefficients for Compound	$°C^{-1}$, $°C^{-1}$ and °C

3.3. Surface Effects

In constant temperature systems there is often a significant boundary layer, often referred to as a Knudsen layer. In the case presented here, the temperature increases to the point of equilibrium between radiation, mass ejection and thermal conduction (for the time dependent case). Boundary layer effects are thus different as there is a source of additional power (the directed energy beam) that increases the temperature until equilibrium is reached. In an extreme case a Knudsen layer could completely prevent mass ejection while for a directed energy system this cannot happen unless the temperature rises to the point of complete radiation balance. For flux levels near 10 $\mathrm{MW/m^2}$ this would be greater than 6 000 K. Thus the boundary layer is greatly mitigated by the constant directed energy impinging on the target. . A related effect would be the scattering and reflection at a boundary layer that would prevent the beam from reaching the surface. This latter effect tends to be quite small given the relatively low density of the plume. The coefficient of evaporation is another related surface effect which is different in the case of a directed energy system as the spot temperature will rise until the material is ejected. In the current analysis these effects are neglected, and future work will address this issue.

3.4. Vapor Pressure

The vapor pressure of each element or compound can be computed from its associated Antoine coefficients (A, B, C). Based on the computed vapor pressures, the mass ejection flux can be determined for the full 3D and 4D cases numerically.[3] Note that in most cases, the Antoine coefficients are computed for Celsius temperature, and pressures are reported in mm Hg:

$$\left(P_v\right)_{Hg} = 10^{\left[\frac{A-B}{(T)_C - C}\right]} \tag{10}$$

The mass ejection flux is computed as:

$$\left|\overline{F}_{Ejecta}\right| = \Gamma_e H_{eff} = M^{1/2}(2\pi RT)^{-1/2}\alpha_e 10^{[A-B/(T+C)]} H_{eff} \tag{11}$$

$$\left|\overline{F}_L\right| = \left|\overline{F}_{rad}\right| + \left|\overline{F}_{Ejecta}\right| + \left|\overline{F}_{cond}\right| \tag{12}$$

Assuming a Gaussian laser of power L_P, the (radial) laser flux is given by:

$$\left|\overline{F}_L\right| = \frac{L_P}{2\pi\sigma^2} e^{-r^2/2\sigma^2} \tag{13}$$

where r is the distance from the spot center. In numerical solutions, the full 4D (time dependent) case is solved, using:[3]

$$\overline{F}_L = \frac{-P_T}{2\pi\sigma^2} e^{-r^2/2\sigma^2}\hat{n} \tag{14}$$

$$\overline{F}_{rad} = \sigma T^4 \hat{n} \tag{15}$$

$$\overline{F}_{Ejecta} = \Gamma_e H_{eff}\hat{n} = M^{1/2}(2\pi RT)^{-1/2}\alpha_e 10^{[A-B/(T+C)]} H_{eff}\hat{n} \tag{16}$$

4. PHYSICS OF MOLECULAR LINE ABSORPTION

4.1. Absorption Lines

As a laser beam strikes the surface of a target, two important things happen. The surface is heated, creating a blackbody source; and, material is ejected from the surface into the surrounding space. A mass ejecta cloud forms in the space between the laser source and the target, providing an opportunity to observe the molecular absorption lines as the blackbody energy passes through the ejecta cloud. Typically, during evaporation or sublimation, the material coming off the target is not ionized and the spot temperatures are low enough that infrared vibrational and rotational lines are observed.[24,25] The computed and measured absorption lines can be used to determine the observed spectra, as follows. At the surface of the spot:

$$B(\lambda)\ (w/m^2 - m) = c\rho(\lambda)/4 \tag{17}$$

$$F(\lambda)\ (w/m^2 - st - m) = B(\lambda)/\pi = c\rho(\lambda)/4\pi \tag{18}$$

$$N(\lambda)\ (\gamma/m^2 - s - st - m) = F(\lambda)/hv \tag{19}$$

where $F(\lambda)/hv$ is the photon flux at the surface of the spot. Symbols used in equations and text in this section are defined in Table 2. The spectral absorption lines due to molecular absorption can be calculated. The ejecta density, in molecules per cubic meter, is given by:

$$n'(z,R) = \frac{4\Sigma}{v}[(1-(R^2/z^2+1)^{-1/2}] \tag{20}$$

Where Σ is the ejecta flux, in molecules $m^{-2}\ s^{-1}$ from the spot. The observed photon rate received per unit bandwidth by the telescope $G(\lambda)$ in $\gamma\ s^{-1}\ m^{-1}$ is calculated form the observed photon flux at the telescope $H(\lambda)$ and the spot area of the asteroid:

$$G(\lambda) = H(\lambda)\cdot A_T \tag{21}$$

Let $\sigma(\lambda)$ be absorption cross section (in m^2 atom^{-1}), then the observed photon rate is:

$$G(\lambda) = A_{spot}N(\lambda)\Omega_T \exp[-\int_0^L n'(z,R)\sigma(\lambda)dz] = A_{spot}N(\lambda)\Omega_T e^{-\tau(\lambda)} \tag{22}$$

Then, $\tau(\lambda)$ is the integrated absorption line coefficient:

$$\sigma(\lambda)\int_0^L n'(z,R)dz \tag{23}$$

and the observed photon rate is:

$$G(\lambda) = \frac{A_{spot}A_T}{4\pi L^2}N(\lambda)\exp[-\int_0^L n'(z,R')\sigma(\lambda)dz] = \frac{A_{spot}A_T}{4\pi L^2}N(\lambda)e^{-\tau(\lambda)} \tag{24}$$

Table 2. Terms used in equations and text in Section 4.

Symbol	**Interpretation**	**Units**
$n'(z, R)$	Ejecta Density at distance z and radial location R	atoms m^{-3}
R	Spot radius on asteroid	m
λ	Wavelength	m
Σ	Ejecta flux	atoms $m^{-2}\ s^{-1}$
$\sigma(\lambda)$	Absorption cross section	m^2 atoms^{-1}
$H(\lambda)$	Observed photon flux at telescope	$\gamma\ m^{-2}\ s^{-1}\ m^{-1}$
$G(\lambda)$	Observed photon rate received per unit bandwidth by telescope	$\gamma\ s^{-1}\ m^{-1}$
$N(\lambda)$	Spectral radiance emitted at the spot	$\gamma\ m^{-2}\ s^{-1}\ sr^{-1}\ m^{-1}$
$B(\lambda)$	Power emitted at the spot	W $m^{-2}\ s^{-1}$
$\rho(\lambda)$	Spectral density at the spot	J $m^{-3}\ m^{-1}$
$F(\lambda)$		W $m^{-2}\ sr^{-1}\ m^{-1}$
A_{Spot}	Spot area of asteroid = $\pi\cdot R^2$	m^2
A_T	Telescope area	m^2
L	Distance to asteroid	m
Ω_T	Solid angle of telescope as viewed from asteroid = $A_T/(4\cdot\pi\cdot L^2)$	sr
$\tau(\lambda)$	Integrated absorption line coefficient (optical depth)	
Γ_ε	Ejected mass flux (from Eq. (9))	kg $m^{-2}\ s^{-1}$
n_0	Surface spot density	atoms m^{-3}

The ejecta flux can be determined as a number of particles:

$$\Sigma(\#/m^2 s^{-1}) = \Gamma_e (kg(m^2 s^{-1})/m) \tag{25}$$

Note that the ejecta density at some distance z from the asteroid and a radial location R is given by:

$$n'(z,R) = \frac{4\Sigma'(z)}{v} = \frac{4\Sigma}{v}[1-(R^2/z^2+1)^{-1/2}] \tag{26}$$

and that the following asymptotic relationships with distance hold:

$$n'(z,R) \to \frac{4\Sigma}{v} \ as\, z \to 0, \quad \text{and} \quad n'(z,R) \to \frac{2\Sigma R^2}{vz^2} \ as\, z \to \infty \tag{27}$$

The integrated absorption line coefficient as a function of wavelength is found by:

$$\tau(\lambda) = \sigma(\lambda)\int_0^L n'(z,R)dz = \frac{4\Sigma\sigma(\lambda)}{v}\int_0^L [1-(R^2/z^2+1)^{-1/2}]dz \tag{28}$$

Using the asymptotic relationships:

$$\int_0^L \left[1-\left(R^2/z^2\right)^{-1/2}\right]dz = L-(R^2+L^2)^{1/2}+R \to R \ \text{ as } \ L \to \infty \tag{29}$$

and:

$$\tau(\lambda) = \frac{4\Sigma\sigma(\lambda)}{\upsilon}R \ \text{ as } \ L \to \infty \tag{30}$$

Giving the observed photon rate received per unit bandwidth by telescope as:

$$G(\lambda) = \frac{A_{spot}A_T}{4\pi L^2}N(\lambda)e^{-\tau(\lambda)} = \frac{A_{spot}A_T}{4\pi L^2}N(\lambda)e^{-(4\Sigma\sigma(\lambda)R/\upsilon)} \tag{31}$$

And the observed photon flux at the telescope as:

$$H(\lambda) = G(\lambda)/A_T = \frac{A_{spot}}{4\pi L^2}N(\lambda)e^{-(4\Sigma\sigma(\lambda)R/\upsilon)} \tag{32}$$

The absorption coefficient as a function of wavelength $\tau(\lambda)$ is given by:

$$\tau(\lambda) = n\sigma(\lambda)X = \frac{4\Sigma\sigma(\lambda)}{\upsilon}R \tag{33}$$

where n is an effective density and X is an effective length, the following relationships hold:

$$n = \frac{4\Sigma}{\upsilon} \ \text{ and } \ X = R \tag{34}$$

These relationships are reasonable, since it follows that $\Sigma = n \cdot v/4$ which makes sense. The effective length $X = R$, which is just the spot radius, hence:

$$\tau(\lambda) = n\sigma(\lambda)R \tag{35}$$

4.2. Spectrometry

It is now possible to compute the observed spectrum (rate received) G(λ) ($\gamma\ s^{-1}\ m^{-1}$) and (flux received) H(λ) (γ m-^{2} s^{-1} m^{-1}) as measured by a spectrometer as follows:

$$H(\lambda) = \frac{G(\lambda)}{A_T} \tag{36}$$

$$\Omega_T = \frac{A_T}{4\pi L^2} \tag{37}$$

Assuming the heated spot is a blackbody with temperature T for simplicity, with spectral radiance of $N_\lambda = N(\lambda)$ emitted at the spot, then the spectral power emitted at the spot is:

$$B_\lambda = \frac{c\rho_\lambda}{4} = \frac{2\pi hc^2}{\lambda^5 \cdot (e^{hc/\lambda kT} - 1)} \tag{38}$$

The spectral density at the spot is:

$$\rho_\lambda = \frac{8\pi hc}{\lambda^5 \cdot (e^{hc/\lambda kT} - 1)} \tag{39}$$

$$F_\lambda = \frac{c\rho_\lambda}{4\pi} = \frac{2hc^2}{\lambda^5 \cdot (e^{hc/\lambda kT} - 1)} \tag{40}$$

$$N_\lambda = \frac{F_\lambda}{hv} = \frac{F_\lambda \lambda}{hc} = \frac{2c}{\lambda^4 \cdot (e^{hc/\lambda kT} - 1)} \tag{41}$$

$$B_\lambda = \pi F_\lambda \tag{42}$$

It is now possible to calculate the observed spectra $G(\lambda)$:

$$G_\lambda = N(\lambda) A \Omega_T e^{-\tau(\lambda)} \tag{43}$$

where the optical depth and surface spot density are:

$$\tau(\lambda) = 4\Sigma \sigma(\lambda) R / \upsilon = n_0 \sigma(\lambda) R \tag{44}$$

$$n_0 = 4\Sigma / \upsilon \tag{45}$$

The calculated cross sections for two molecular species, water and silica (SiO), are shown as examples in Fig. 4.

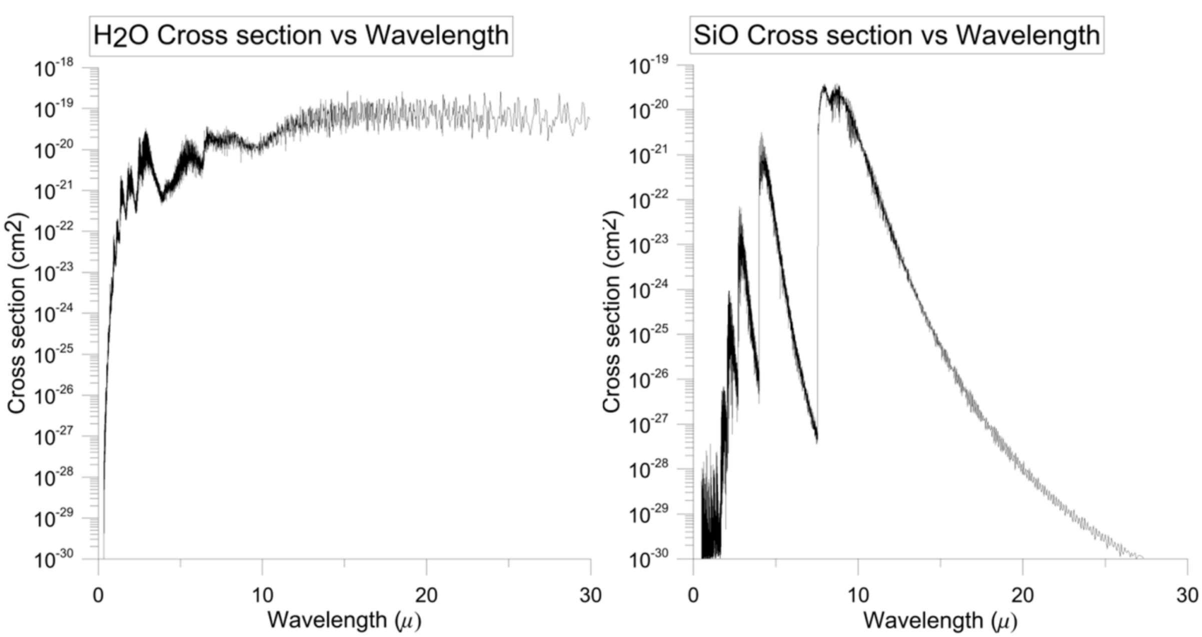

Figure 4. Cross section vs. wavelength for Water and Silica (SiO).

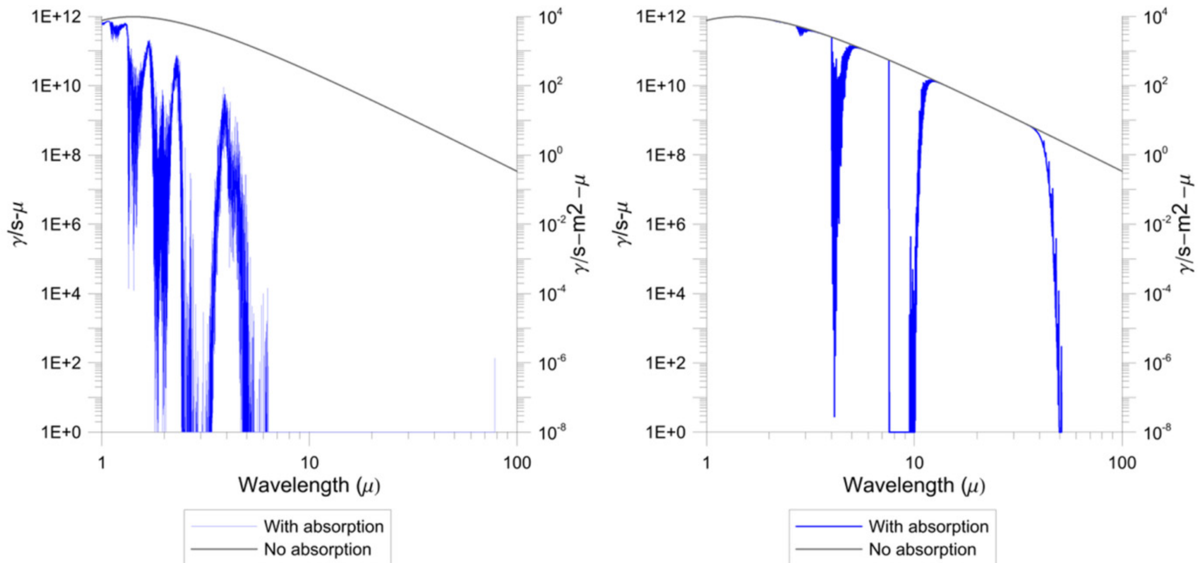

Figure 5. Predicted Spectra for water (left) and SiO (right) for the a DE-STAR 4 system at 1 AU.[3]

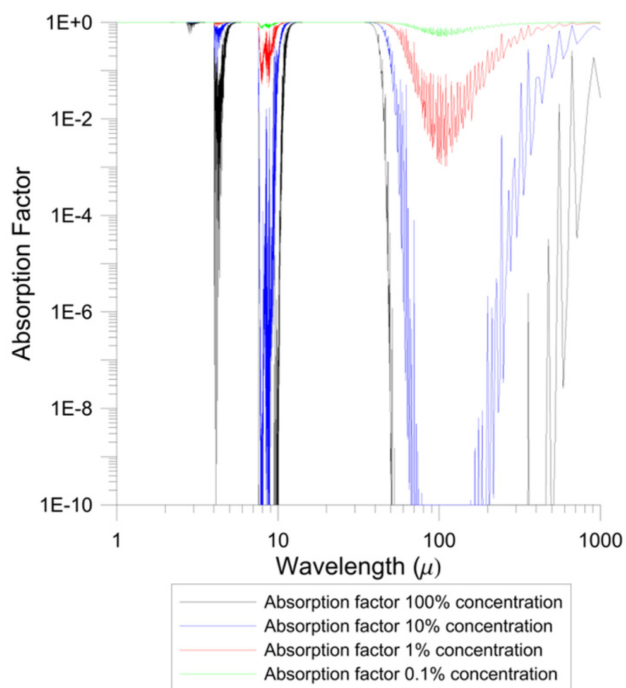

Figure 6. Since an asteroid will not be completely made of SiO, the absorption spectrum is computed for fractional compositions of 0.1 to 100% SiO to give an indication of the sensitivity to fractional composition. The "absorption factor" is the fractional composition of SiO.

5. CONCLUSIONS

Laser-induced mass ejection can be used to remotely interrogate the composition of a distant target. The feasibility of such a measurement depends on the details of the molecular cross section of the material in question and the laser power and distance to the target. Examples described in this paper indicate the possible sensitivity of this method for long range detection. The determination of the composition of asteroids and other targets allows for future resource extraction by pre determining the materials in the target before visiting it. This is one example of the system. More materials are being investigated for remote analysis as are various system designs to determine practical methods of carrying out such surveys. Resource extraction in the solar system will become increasingly important and standoff molecular composition analysis is one method to aid in this endeavor.

ACKNOWLEDGEMENTS

We gratefully acknowledge funding from the NASA California Space Grant NASA NNX10AT93H in support of this research.

REFERENCES

[1] Bernath, P.F. "Molecular Astronomy of Cool Stars and Sub-Stellar Objects," *International Reviews in Physical Chemistry*, 28:4, pp. 681-709 (2009).

[2] Bernath, P.F. *Spectra of Atoms and Molecules, Second Edition*. New York: Oxford University Press, 439 p., ISBN 9780195177596 (2005).

[3] Lubin, P., Hughes, G.B., Bible, J., Bublitz, J., Arriola, J., Motta, C., Suen, J., Johansson, I., Riley, J., Sarvian, N., Clayton-Warwick, D., Wu, J., Milich, A., Oleson, M., Pryor, M., Krogen, P., Kangas, M., and O'Neill, H. "Toward Directed Energy Planetary Defense," *Optical Engineering*, Vol. 53, No. 2, pp 025103-1 to 025103-18 (Feb. 2014), doi: 10.1117/1.OE.53.2.025103.

[4] Miziolek, A.W., Palleschi, V., and Schechter, I. (Eds.). *Laser Induced Breakdown Spectroscopy (LIBS): Fundamentals and Applications*. New York: Cambridge University Press, ISBN 978-0-521-85274-6 (2006).

[5] Demtröder, W. *Laser Spectroscopy: Basic Concepts and Instrumentation*. New York: Springer Science & Business Media, 986 p., ISBN 978-3-662-05155-9 (2013).

[6] Brophy, J.R. and Muirhead, B. "Near-Earth Asteroid Retrieval Mission (ARM) Study," *Proc. of the 33rd International Electric Propulsion Conference*, IEPC-2013-082, (Oct. 2013).

[7] Colombo, C, Vasile, M. and Radice, G. (2009). "Semi-Analytical Solution for the Optimal Low-Thrust Deflection of Near-Earth Objects." *Journal of Guidance, Control, and Dynamics* 32.3: 796-809.

[8] Gibbings, M. A., Hopkins, J. M., Burns, D., & Vasile, M. (2011). "On Testing Laser Ablation Processes for Asteroid Deflection." *2011 IAA Planetary Defense Conference*, Bucharest, Romania.

[9] Zhang, Q., Walsh, K., Mellis, C., Hughes, G.B., Lubin, P. "Orbital Simulations of Directed Energy Deflection of Near-Earth Asteroids" to be published in *Proceedings of the 13th Hypervelocity Impact Symposium* (in press, 2015).

[10] Lubin, P. and Hughes, G.B. "Directed Energy for Planetary Defense." Chapter in: Allahdadi, Firooz, and Pelton, Joseph N. (Eds.), *Handbook of Cosmic Hazards and Planetary Defense*, Springer Reference, ISBN 978-3-319-03951-0 (2015).

[11] Bible, J., Bublitz, J., Johansson, I., Hughes, G.B., and Lubin, P. (2013). "Relativistic Propulsion Using Directed Energy," *Nanophotonics and Macrophotonics for Space Environments VII*, edited by Edward W. Taylor, David A. Cardimona, Proc. of SPIE Vol. 8876, 887605.

[12] Riley, J., Lubin, P., Hughes, G.B., O'Neill, H., Meinhold, P., Suen, J., Bible, J., Johansson, I., Griswold, J. and Cook, B. "Directed energy active illumination for near-Earth object detection," *Journal of Astronomical Telescopes, Instruments and Systems*. (in Review, 2015)

[13] Riley, J., Lubin, P., Hughes, G.B., O'Neill, H., Meinhold, P., Suen, J., Bible, J., Johansson, I., Griswold, J. and Cook, B. "Directed energy active illumination for near-Earth object detection," *Nanophotonics and Macrophotonics for Space Environments VIII*, edited by Edward W. Taylor, David A. Cardimona, Proc. of SPIE Vol. 9226 (Aug. 2014).

[14] Zervas, M.N. and Codemard, C.A. "High power fiber lasers: a review." *IEEE Journal of Selected Topics in Quantum Electronics*, vol. 20, no. 5, pp. 219-241 (2014).

[15] Wagner, T.J. "Fiber laser beam combining and power scaling progress: Air Force Research Laboratory Laser Division." *SPIE LASE*, pp. 823718-823718. Proc. of SPIE vol. 8237 (Feb. 2012).

[16] Vorontsov, M.A., Weyrauch, T., Beresnev, L.A., Carhart, G.W., Liu, L. and Aschenback, K. "Adaptive Array of Phase-Locked Fiber Collimators: Analysis and Experimental Demonstration," *IEEE Journal of Selected Topics in Quantum Electronics*, vol. 15, 269 (2009).

[17] Liu, H., He, B., Zhou, J., Dong, J., Wei, Y., & Lou, Q. "Coherent beam combination of two nanosecond fiber amplifiers by an all-optical feedback loop." *Optics Letters*, *37*(18), 3885-3887 (2012).

[18] Su, R., Zhou, P., Wang, X., Zhang, H., & Xu, X. "Active coherent beam combining of a five-element, 800 W nanosecond fiber amplifier array." *Optics Letters*, *37*(19), 3978-3980 (2012)

[19] Yu, C.X., Augst, S.J., Redmond, S.M., Goldizen, K.C., Murphy, D.V., Sanchez, A., and Fan, T.Y. "Coherent combining of a 4 kW, eight-element fiber amplifier array." *Optics Letters*, 36(14), 2686-2688 (2011).

[20] Steffanic, P., Johannes, B.T., Sison, C.A., Hughes, G.B., Lubin, P., Meinhold, P., Suen, J., O'Neill, Kangas, M., Brashears, T., Zhang, Q., Griswold, J., Riley, J., and Motta, C. "Local phase control for a planar array of fiber laser amplifiers," *Nanophotonics and Macrophotonics for Space Environments IX*, edited by Edward W. Taylor, David A. Cardimona, Proc. of SPIE Vol. 9616 (Aug. 2015).

[21] Kosmo, K., Pryor, M., Lubin, P., Hughes, G.B., O'Neill, H., Meinhold, P., Suen, J., C., Riley, J., Griswold, J., Cook, B.V., Johansson, I.E., Zhang, Q., Walsh, K., Melis, C., Kangas, M., Bible, J., Motta, Brashears, T., Mathew, S. and Bollag, J. "DE-STARLITE - a practical planetary defense mission," *Nanophotonics and Macrophotonics for Space Environments VIII*, edited by Edward W. Taylor, David A. Cardimona, Proc. of SPIE Vol. 9226 (Aug. 2014).

[22] Hughes, G.B., Lubin, P., Bible, J., Bublitz, J., Arriola, J., Motta, C., Suen, J., Johansson, I.E., Riley, J., Sarvian, N., Wu, J., Milich, A., Oleson, M., and Pryor, M. "DE-STAR: phased-array laser technology for planetary defense and other scientific purposes," *Nanophotonics and Macrophotonics for Space Environments VII*, edited by Edward W. Taylor, David A. Cardimona, Proc. of SPIE Vol. 8876, 88760J (Aug. 2013).

[23] Kosmo, K., Lubin, P., Hughes, G.B., Griswold, J., Zhang, Q. and Brashears, T. "Directed Energy Planetary Defense," *Aerospace Conference 2015 IEEE Proceedings*, 7-14 March 2015, ISBN: 978-1-4799-5379-0 (Mar. 2015).

[24] Barton, E. J., Yurchenko, S. N., and Tennyson, J. "ExoMol line lists–II. The Ro-Vibrational Spectrum of SiO," *Monthly Notices of the Royal Astronomical Society*, vol. 434(2), pp. 1469-1475 (2013)

[25] Tennyson, J. and Yurchenko, S.N. "ExoMol: molecular line lists for exoplanet and other atmospheres," *Monthly Notices of the Royal Astronomical Society* vol. 425, pp. 21-33 (2012).

[26] Hill, C., Yurchenko, S.N. and Tennyson, J. "Temperature-dependent molecular absorption cross sections for exoplanets and other atmospheres," *Icarus* vol. 226, pp. 1673-1677 (2013).